Title: Articular cartilage corefucosylation regulates tissue resilience in osteoarthritis

Short title: Articular cartilage corefucosylation and tissue resilience in OA

Kentaro Homan[1], Tomohiro Onodera[1]*, Hisatoshi Hanamatsu[2], Jun-ichi Furukawa[1, 2], Daisuke Momma[3], Masatake Matsuoka[1], Norimasa Iwasaki[1]

[1] Department of Orthopaedic Surgery, Faculty of Medicine and Graduate School of Medicine, Hokkaido University, Kita 15, Nishi 7, Kita-ku, Sapporo 060-8638, Japan

[2] Institute for Glyco-core Research (iGCORE), Nagoya University, Nagoya 464-8601, Japan

[3] Center for Sports Medicine, Hokkaido University Hospital, Kita 14, Nishi 5, Sapporo 060-8638, Japan.

*Corresponding author: Tomohiro Onodera

Department of Orthopaedic Surgery, Faculty of Medicine and Graduate School of Medicine

Hokkaido University, Kita 15, Nishi 7, Kita-ku, Sapporo 060-8638, Japan

Telephone: +81-11-706-2111

Email: tomozou@med.hokudai.ac.jp

Abstract

This study aimed to investigate the glycan structural changes that occur before histological degeneration in osteoarthritis (OA) and to determine the mechanism by which these glycan conformational changes affect cartilage degeneration. An OA model was established in rabbits using mannosidase injection, which reduced high-mannose type N-glycans and led to cartilage degeneration. Further analysis of glycome in human OA cartilage identified specific corefucosylated N-glycan expression patterns. Inhibition of N-glycan corefucosylation resulted in unrecoverable cartilage degeneration, while cartilage-specific blocking of corefucosylation led to accelerated development of aging-associated and instability-induced OA models. We conclude that α1,6 fucosyltransferase is required postnatally to prevent preosteoarthritic deterioration of articular cartilage. These findings provide a novel definition of early OA and identify glyco-phenotypes of OA cartilage, which may distinguish individuals at higher risk of progression.

Keywords: early osteoarthritis, glyco-phenotypes, α1,6 fucosyltransferase, cartilage glycome

INTRODUCTION

Osteoarthritis (OA), a degeneration of joint components, such as proteoglycans (PGs) and collagen, destroys cartilage and impairs joint function (1). The global prevalence of OA is estimated to be >500 million, which is a significant socioeconomic burden (2). Therefore, preventive measures must be implemented to reduce the future disease burden and disability. Once the cartilage is destroyed, it cannot be repaired homogeneously and progresses irreversibly thereafter (3, 4). Since articular cartilage has no blood vessels and is not innervated, it is difficult for symptoms to appear. By the time clinical symptoms appear, the condition is often already considerably advanced (5). Therefore, from a preventive

46 perspective, it is necessary to define and detect "pre-OA," the stage before the onset of early
47 OA (6, 7). Pre-OA is a knee with no pain, no motor function problems, and no arthroscopic or
48 structural changes on radiography, only emerging cellular effects. Despite many studies, there
49 is no gold standard for OA biomarkers (8). It is important to characterize the disease state
50 before OA to shift the paradigm from mitigation to late-onset disease prevention.
51 In the very early stages of OA, before cartilage matrix degeneration, cartilage destruction by
52 enzymatic processes that degrade glycoproteins, PGs, and collagen, in that order, is underway
53 (9). Collagenolytic activity is largely unchanged on intact articular surfaces (10, 11), and
54 glycoprotein degradation is thought to be an early transient event in the enzymatic process of
55 cartilage destruction because hexose degradation of glycoproteins promotes degradation of
56 the protein portion of the molecule by proteinases (12). Additionally, cartilage damage is
57 reversible if type 2 collagen breakdown is mild (13). Structural change analysis in
58 glycoproteins is necessary for the early stages of OA but has not yet been performed
59 sufficiently.
60 Matsuhashi *et al*.'s study showed that structural changes in N-glycans occurred in
61 degenerated cartilage in a rabbit OA model before tissue changes occurred (14). Urita *et al*.
62 demonstrated that these N-glycans in degenerated mice and human cartilage are high-
63 mannose type N-glycans (15). Furthermore, among several glycosidases, mannosidase
64 activity was very high in OA joints, and its activity was high before the progression of
65 cartilage fibrosis (16). This suggests that high-mannose type N-glycan plays an important
66 role in OA pathogenesis. However, whether changes in the glycan structure are involved in
67 OA pathogenesis is unclear.
68 This study analyzed the glycan structural changes that preceded OA degeneration and
69 elucidated the mechanism of glycan structural changes in cartilage degeneration. For this
70 purpose, the effects of mannosidase, a specific degrading enzyme of high-mannose type N-

71 glycans associated with OA, on cartilage tissues and its molecular mechanisms were
72 analyzed.
73
74 **RESULTS**
75 **Mannosidase injection caused early OA-like change in vivo**
76 A decrease in Safranin O staining in the right femoral condyle of the α-mannosidase-injected
77 knee after 4 weeks was observed (Fig. 1A, B). Terminal deoxynucleotidyl transferase dUTP
78 nick end labeling (TUNEL) staining was enhanced in the superficial layer compared with that
79 in control. Articular cartilage chondrocytes exposed to α-mannosidase were not arranged in
80 columns in the middle zone. The surfaces of each group were smooth and had a good
81 macroscopic appearance (Fig. 1C). None of the groups showed a decrease in type 2 collagen
82 staining, and the orientation was maintained (Fig. 1D). To achieve optimal activity, the pH
83 range of 4 to 5 is ideal for mannosidase. In a physiological saline solution with a pH of 7 and
84 a concentration of 100 μg/ml, it exhibited specific activity. Nevertheless, at a concentration of
85 1.0 μg/ml, this activity was no longer present (S1 Figure). The mean histological score of the
86 α-mannosidase group was 0.83, indicating mild OA (Fig. 1E). The control group was
87 unchanged. Cartilage degeneration during intermittent intra-articular administration of
88 mannosidase was reversed upon discontinuation (Fig. 1F).
89
90 **Depletion of high-mannose type N-glycans in chondrocytes leads to cartilage**
91 **degradation ex vivo**
92 To quantify the degeneration and resilience promoted by the injection of α-mannosidase, the
93 cultured cartilage was harvested at different time points (Fig. 2A). Concanavalin A (Con A)
94 reactivity declined in articular cartilage treated with α-mannosidase (Fig. 2B). The
95 application of α-mannosidase stimulated the release of PG from cultured cartilage in

96 association with extracellular matrix degradation (Fig. 2C) and showed significantly higher
97 spontaneous nitric oxide (NO) release than the control over time (Fig. 2F). Mannosidase-
98 exposed cartilage showed an increase in TUNEL-positive cells in chondrocytes in the deep
99 zone and type 10 collagen-positive cells in superficial chondrocytes; however, these changes
100 did not occur in cytokine-stimulated cartilage (S2 Figure). Mannosidase exposure increased
101 *Adamts5* expression and suppressed *Mmp13* expression and anabolic factors (Fig. 3E). In the
102 articular cartilage that was exposed to freeze-thaw treatment before culture, no differences in
103 PG loss were observed between the α-mannosidase-stimulated cartilage and non-stimulated
104 cartilage (Fig. 2E). Excluding mannosidase loading, PG leakage and Safranin O staining were
105 restored (Fig. 2D), but Con A staining loss was not. Sialidase addition did not cause PG
106 leakage or NO production (S3 Figure), and the aggrecan lost in the catabolic phase was not
107 replenished in the subsequent anabolic phase.
108
109 **Corefucosylated N-glycan was formed in resilient cartilage**
110 Glycoblotting analysis revealed a significant difference in the N-glycan profiles (Fig. 3A and
111 S1 Table). Plotting m/z after mannosidase exposure against m/z before mannosidase exposure
112 demonstrated that only N-glycans were affected by enzyme dissociation from the y = x line
113 (Fig. 3B, S2 Table). In both denatured and reverted cartilages, Man8-9GlcNAc2 was
114 decreased, and Man5-6GlcNAc2 was increased by the action of mannosidase, which has a
115 high specificity for the terminal mannosidic residues of glycans (Fig. 3C, D). In contrast,
116 corefucosylated N-glycans, which were formed in the same biosynthesis pathway, were also
117 found (Fig. 3D). Similarly, the N-glycan profiles of isolated chondrocytes showed the
118 presence of this corefucosylated structure (S4 Figure). The expression of *Fut8*, the only
119 enzyme involved in corefucosylation, increased significantly in mannosidase-treated cartilage
120 (Fig. 3E).

121

122 **Deficiency of corefucosylated glycans in articular cartilage inhibits recovery from**

123 **cartilage damage and promotes cartilage degeneration**

124 We first examined whether the absence of core fucose affects the resilience of cartilage

125 degeneration. Mice lacking *Fut8* exhibited severe growth retardation and died shortly after

126 birth. Therefore, we decided to generate *Fut8* conditional knockout (cKO) mice (Fig. 4A, B).

127 The tissue specificity of recombination was confirmed by polymerase chain reaction (PCR)

128 analysis of mouse genomic DNA that detected either the intact $Fut8^{loxP}$ allele or the Cre-

129 recombined $Fut8^{\Delta}$ allele in repeated crosses; N-glycan analysis of cartilage demonstrated the

130 loss of corefucosylated sugar chains (Fig. 4C). The proportion of high-mannose type N-

131 glycan content was unchanged in cartilage lacking the *Fut8* gene (S5 Figure). Next, we used

132 real-time (RT)-PCR to determine relative *Fut8* messenger (m)-RNA levels in the cartilage of

133 Col2-$Fut8^{-/-}$ mice and their wild-type (WT) littermates ($Fut8^{loxP/loxP}$). Real-time polymerase

134 chain reaction (RT-PCR) analysis showed that *Fut8* mRNA expression was reduced by >99%

135 in the articular cartilage of Col2-$Fut8^{-/-}$ mice compared to that in their WT littermates ($P <$

136 0.01; $n = 3$ mice per group) (Fig. 4D). Chondrocyte-surface corefucosylation levels were

137 analyzed by lectin staining using *Pholiota squarrosa* lectin (PhoSL), which specifically

138 recognizes α1-6 core fucose (17). PhoSL lectin staining was completely absent in the articular

139 cartilage of *Fut8* cKO mice, in contrast to the positive staining observed in *Fut8* flox mice

140 under physiological conditions (Fig. 4E). Enzymatic degradation of high-mannose type N-

141 glycans on the cartilage in *Fut8*-deficient mice exacerbated cartilage degeneration (Fig. 4E,

142 F). In addition, reversible matrix repair by enzyme removal observed in control cartilage was

143 not observed in *Fut8*-deficient cartilage explant cultures.

144

145 **Loss of corefucosylated glycans in articular cartilage leads to premature OA**

146 Col2-*Fut8*$^{-/-}$ mice developed and grew normally without major organ abnormalities of major
147 organs and could not be distinguished from their WT littermates. The whole skeletons of
148 newborn mice stained with alcian blue and alizarin red did not differ in appearance between
149 the genotypes (Fig. 5A). Col2-*Fut8*$^{-/-}$ mice showed a lower body weight than their WT
150 littermates, as indicated by the growth curve (Fig. 5B). We analyzed the development of
151 instability-induced OA changes in *Fut8*$^{\mathrm{loxP/loxP}}$ and *Fut8* cKO mice. Sham operations
152 produced no significant changes in OA in either mouse genotype. Eight weeks after
153 instability-inducing surgery, the joints of WT mice developed changes in OA, such as
154 cartilage erosion and a reduction in Safranin O staining and chondrocyte number. Deletion of
155 FUT8 results in more severe changes in OA. In the joints of *Fut8* cKO mice, 8 weeks after
156 surgery, the noncalcified zone (upper layer above the tidemark) was almost completely lost.
157 The number of chondrocytes was significantly reduced (Fig. 5C). Quantitative assessment
158 using the OA Research Society International (OARSI) score supported these histological
159 findings (difference: -2.900; *Fut8*$^{flox/flox}$/destabilization of the medial meniscus (DMM) versus
160 *Col2a1-Cre*; *Fut8*$^{flox/flox}$/DMM, 95% confidence interval [CI] for the difference: -5.027 to -
161 0.7734) (Fig. 5D). Changes in OA progressed earlier in the aging models of *Fut8*-deficient
162 mice than in control mice (WT and floxed mice). The mice were followed up until 15 months
163 of age to assess the spontaneous development of OA with aging (Fig. 5E). There were no
164 apparent changes of OA in the knee joints of either mouse genotype at 3 months of age (Fig.
165 5F). At 4 months of age, significant changes in OA were detected in the knee joints of the
166 *Fut8* cKO mice. The cartilage surface integrity was no longer maintained at 9 months. These
167 OA changes progressed more in *Fut8* cKO mice than in their WT littermates at 15 months.
168 These histological findings were quantitatively confirmed by the Osteoarthritis Research
169 Society International (OARSI) scores (difference: -2.000; WT versus *Col2a1-Cre; Fut8*$^{flox/flox}$,

170 95% CI for the difference: -3.723 to -0.2771 at 4 months, difference: -2.700; WT versus
171 *Col2a1-Cre; Fut8*$^{flox/flox}$, 95% CI for the difference: -4.423 to -0.9771 at 9 months, and
172 difference: -6.700; WT versus *Col2a1-Cre; Fut8*$^{flox/flox}$, 95% CI for the difference: -8.423 to -
173 4.977 at 15 months).
174
175 **Altered glycosylation of human OA cartilage based on comprehensive glycan analysis**
176 Total glycome profiling of human OA cartilage is shown in Fig. 6A and S3 Table. The
177 amount of high-mannose type N-glycan was significantly decreased, the same as previously
178 reported in OA cartilages (Fig. 6A) (15). Focusing on fucosylation, most of the
179 complex/hybrid type glycans were modified with fucose. The fucosylation that occurs at the
180 innermost N-acetylglucosamine (GlcNAc) of N-glycans could be recognized with a lectin
181 from the mushroom Pholiota squarrosa (PhoSL) and was able to detect the expression of the
182 corefucose structure. Therefore, we suspected that the stainability of PhoSL is increased in
183 OA cartilage. As expected, the PhoSL staining of OA cartilage was significantly increased
184 relative to that of a healthy control (Fig. 6B). We performed principal component analysis
185 (PCA) on 1110 glycomic data, discriminating OA from healthy cartilages along the first
186 principal component (PC1) axis (Fig. 6C). Hierarchical cluster analysis showed that clades
187 containing corefucosylated glycans were clustered (Fig. 6D), and N-13 ((Hex)1 (HexNAc)1
188 (Fuc)1 + (Man)3(GlcNAc)2) has the largest squared correlation with its cluster component.
189
190 **DISCUSSION**
191 To test the hypothesis that structural changes in high-mannose type N-glycans may induce
192 OA, we tested the effect of mannosidase loading on the structure of high-mannose type N-
193 glycans. Consequently, modifying the structure of high-mannose type N-glycans by
194 mannosidase loading induced OA-like histological alterations. Furthermore, the OA-like

195 changes induced by mannosidase were recovered by enzyme removal. These results suggest
196 that structural alterations of high-mannose type N-glycans lead to OA-like histological
197 changes in articular cartilage but do not necessarily cause the pathogenesis of eventual OA.
198 Subsequently, glycoblotting analysis revealed that core-fucose-containing glycans underwent
199 complementary structural alterations per high-mannose type N-glycans. This suggests that the
200 structural change of core-fucose-containing glycans may have some compensatory
201 mechanism for OA-like alterations caused by the structural change of high-mannose type N-
202 glycans. Furthermore, under the regulation of *Fut8* expression, which regulates the synthesis
203 of core fucose, mannosidase was found to induce irreversible OA. These results provide the
204 first evidence that structural alterations in glycans in the articular cartilage regulate eventual
205 OA development.
206 Two key targets of cartilage degeneration during OA are type II collagen, a major substrate of
207 matrix metalloproteinase (MMP)-13 (18), and aggrecan, a PG with glycosaminoglycan side
208 chains of chondroitin and keratin sulfate (19, 20). The degradation of non-collagenous
209 molecules, such as aggrecan, occurs before the degradation of type II collagen in the early
210 stages of OA (20, 21). The histological analysis in this study revealed that the alteration in the
211 structure of high-mannose type N-glycans resulted in a decrease in Safranin O staining (a
212 decrease in glycosaminoglycans and/or PGs), whereas there was no change in collagen
213 staining. These findings are consistent with alterations in the early stages of OA.
214 Furthermore, we observed that removing mannosidase could cause PG loss to the control
215 level. Karsdal *et al.* demonstrated that articular cartilage degradation is reversible in the
216 presence of aggrecanase and concluded that the repair ability is not impaired before the
217 degradation of aggrecan and type II collagen by MMPs (22). Reimann *et al.* observed that the
218 glycosaminoglycans loss in articular cartilage is reversible and an early sign of OA before the
219 "state of no return." (23) The present results are consistent with findings of previous reports

220 on early OA and suggest that the mannosidase-loaded model can be considered an early OA-
221 like alteration.
222 Since the structural change in high-mannose type N-glycans alone did not cause irreversible
223 OA, we investigated other regulatory mechanisms related to high-mannose type N-glycans
224 that could induce irreversible OA. The expression of corefucosylated N-glycans on a series of
225 biosynthetic pathways was upregulated with structural changes in high-mannose type N-
226 glycans. FUT8 is known to corefucosylate small oligomannose N-glycans (Man4-
227 Man5GlcNAc2) but not large oligomannose N-glycans, such as Man8-Man9GlcNAc2 (24).
228 This suggests that small oligomannose N-glycans trimmed by mannosidase could activate
229 *Fut8*. *Fut8* is also upregulated in human OA chondrocytes (25, 26), and increased expression
230 of these corefucosylated N-glycans has been observed during late chondrocyte differentiation
231 (27). These findings suggested that these structural changes are related to OA-related
232 glycosylation.
233 To clarify the relationship between the alteration of corefucosylated N-glycans and cartilage
234 degeneration, *Fut8* cKO mice were used. Since the results of the ex vivo freeze-thaw model
235 showed that cartilage degeneration was induced by changes in the glycan structure of
236 chondrocytes, we used chondrocyte-specific KO mice. As a result, the reversibility of the
237 cartilage degeneration model was diminished. This finding suggests that *Fut8*-mediated
238 corefucosylation in chondrocytes plays a function in promoting glycan repair. Furthermore, to
239 directly determine whether *Fut8* was involved in the inhibition of OA progression, an aging
240 model was investigated. The results showed that conditional KO of *Fut8* in chondrocytes
241 hastened the onset of OA. This suggests that cartilage corefucosylation associated with FUT8
242 plays a protective role against the attenuation of type II collagen in the OA process.
243 Finally, the expression of α1,6-linked core fucose on N-glycans in human cartilage is
244 associated with OA, and corefucosylation was found to be one of the characteristics in OA

245 cartilage. Total cellular glycome analysis, including N- and O-linked glycans derived from
246 glycoproteins, GSL-glycans, GAGs, and fOSs, is informative for analyzing cell-specific
247 characteristics (28−30). Glycome profiling enabled the detection of corefucosylated N-
248 glycans by sequential clustering of degenerated cartilage characteristics. Core fucose
249 deficient mice generated by ablating the α1,6 fucosyltransferase enzyme, FUT8, were
250 reported to have suppressed phosphorylation of Smad and increased expression of MMPs
251 (matrix metalloproteinases) due to decreased binding of TGF-β ligand caused by the lack of
252 core fucose addition to the TGF-β type II receptor (31, 32). The present study shows that
253 treatment of cartilage with mannosidase caused corefucosylation, suppression of *Mmp13*, and
254 increased expression of *Tgf-β*. Moreover, treatment of FUT8-knockout cartilage with
255 mannosidase resulted in the suppression of *Tgf-β* expression and increased *Mmp13*
256 expression. These results suggest that corefucosylation following the loss of high-mannose
257 type N-glycans may provide chondroprotective effects via the TGF-β signaling pathway,
258 which may have been lost by FUT8-knockout.
259 One limitation of this study was that we did not have access to cartilage samples from
260 immediately before the onset of OA; thus, we do not know the expression of Fut8 in human
261 cartilage in the early stage of OA onset and its influence on extracellular matrix degradation
262 under homeostatic conditions. Obtaining cartilage specimens continues to be challenging,
263 especially for those with early stages of OA.
264 In summary, we show for the first time a key role of FUT8 and glycan-dependent signaling
265 mediators in extracellular matrix resilience associated with cartilage corefucosylation during
266 early OA.
267

METHODS

Intra-articular injection of α-mannosidase in the knee

Japanese White rabbits weighing 3.10 ± 0.15 kg purchased from a professional breeder (Japan SLC Inc., Hamamatsu, Japan) were used for this study according to established ethical guidelines approved by the local animal care committee. Animals were anesthetized with 10 mg/kg of intravenous ketamine, followed by isoflurane in oxygen gas. Both knees in each rabbit were shaved, prepared, and draped in a sterile fashion. α-Mannosidase from Canavalia ensiformis (Jack bean) (Sigma, St Louis, MO, USA) was dissolved in saline. Five hundred microliter volumes containing 1.9 units per ml (0.05 mg) of mannosidase solution were injected into the joint cavity of the right knee. α-Mannosidase from Canavalia ensiformis (Jack bean) has been widely used as a tool for glycan analysis, which has a high specificity towards terminal mannosidic residues of glycans and participates in mannose trimming reactions (33). The measurement of its performance in a saline solution was evaluated using the QuantiChrom α-Mannosidase Assay Kit (BioAssay Systems, Hayward, CA, USA). This colorimetric assay uses 4-nitrophenyl-α-d-mannopyranoside as a substrate to identify the generation of 4-nitrophenol. The following doses of α-Mannosidase were administered: 0.5 ml at 0.01 μg/ml, 1.0 μg/ml, or 100 μg/ml. Simultaneously, the contralateral knee joint received an equal volume of saline solution. Each joint was injected once or four times in alternate weeks. The animals were euthanized at 4 and 16 weeks postoperatively. Each section of the knee joint was stained with hematoxylin and eosin or Safranin O/fast green, as well as with immunohistochemical staining for type II collagen and TUNEL. Two investigators quantified the OA severity using the OARSI scoring method.

Evaluation of collagen orientation by a polarized light microscope

To evaluate the collagen orientation of the repaired tissue at 16 weeks postoperatively, a

293 supplemental evaluation using a polarized light microscope (PLM) (ECLIPSE E600 POL;
294 Nikon, Tokyo, Japan) was conducted (34). This evaluation was performed on HE-stained
295 sections from each group. Two cross polarizers were used so that highly ordered collagen
296 perpendicular to the articular surface appeared bright, while collagen that was not ordered
297 (nonbirefringent) appeared dark. The contrast of fibrils more parallel to the articular surface
298 was darker than collagen oriented perpendicular to the articular surface. To observe the
299 predominant direction of the birefringent regions and confirm the lack of orientation in the
300 nonbirefringent regions, the sections were rotated at 0°, 45°, and 90° for the fixed filters.
301 Microscopic images were acquired using a digital camera (DS-5M-L1, Nikon, Tokyo, Japan).
302 Each sample was examined independently by an experienced PLM user.
303
304 **Ex vivo analysis of deletion of high-mannose type N-glycan in cartilage**
305 According to the established ethical guidelines approved by the local animal care committee,
306 cartilage catabolism was analyzed by culturing femoral head cartilage of 4-week-old C57BL6
307 male mice with α-mannosidase (1.9 U/mL) ex vivo (35, 36). Mannosidase was removed on
308 day 3, and organ culture was continued until day 6. To evaluate cartilage degradation,
309 quantification of PG release from cartilage explants was performed using the
310 dimethylmethylene blue assay (36, 37) and exposure to sialidase (1.9 U/mL) and interleukin-
311 1 beta (Cat #. 300-01A; BioLegend, San Diego, CA, USA) (10 ng/mL) was also used as
312 another control. The NO concentration in the culture medium was measured using the Griess
313 reagent system (Promega, Tokyo, Japan). To determine the direct effects of mannosidase on
314 the matrix, some cartilage explants were subjected to freeze-thaw cycles in liquid nitrogen to
315 destroy chondrocytes present in the superficial layer of the cartilage (22, 38). After the
316 procedure, the cells were replaced with the same culture medium described above. Each
317 tissue sample was stained with Safranin O. Lectin staining with Con A (Wako Pure Chemical

318 Industries, Richmond, VA, USA) and PhoSL (J-Oil Mills Inc., Tokyo, Japan) was used to
319 detect the high-mannose type N-glycans. Staining was performed using the ABC Kit (Vector
320 Labs, Burlingame, CA, USA), and the sections were counterstained with HE.
321
322 **RNA extraction and quantitative RT-PCR analysis**
323 Total RNA was extracted from the samples using an RNeasy Mini Kit (Qiagen, Hilden,
324 Germany). For complementary DNA synthesis, 1.0 μg of RNA was reverse transcribed using
325 random hexamer primers (Promega, Tokyo, Japan) and ImProm II reverse transcriptase
326 (Promega). Quantitative RT-PCR was performed using a Thermal Cycler Dice Real Time
327 System II (Takara Bio Inc., Otsu, Japan) and SYBR Premix Ex Taq II (Takara, Shiga, Japan)
328 with gene-specific primers (S4 Table) in 15 μl of the mixture, following the manufacturer's
329 instructions. Quantitative data were normalized using peptidylprolyl isomerase A as an
330 endogenous reference gene and were calculated using the ΔΔCt method (39).
331
332 **Generation of *Fut8*$^{loxp/loxp}$*Col2a1-Cre* cKO mice**
333 *Fut8*$^{loxp/loxp}$ mice were provided by Tohoku Pharmaceutical University (Sendai, Japan). To
334 interrupt the synthesis of corefucosylated N-glycans in cartilage, we generated mice with
335 knockout of the chondrocyte-specific *Fut8* gene (Col2-*Fut8*$^{-/-}$ mice) by crossing *Fut8*$^{loxp/lox}$
336 mice with Col2a1-Cre–transgenic mice (40), in which Cre recombinase is expressed
337 specifically in chondrocytes under the Col2a1 promoter. Transgenic mice carrying the
338 Col2a1-Cre transgene (strain B6; SJL-Tg [Col2a1-Cre] 1Bhr/J; stock number 003554) were
339 obtained from the Jackson Laboratory (Bar Harbor, ME, USA). Homozygous *Fut8*$^{loxp/loxp}$
340 mice were bred with *Col2a1-Cre* mice, and offspring with the genotype *Fut8*$^{loxp/+}$ *Col2a1-*
341 *Cre* were bred with *Fut8*$^{loxp/loxp}$ mice to obtain the *Fut8*$^{loxp/loxp}$*Col2a1-Cre* cKO experimental
342 group and *Fut8*$^{loxp/loxp}$ (flox) littermate controls. All animals were maintained at Hokkaido

343 University under the regulations of the Institutional Animal Care and Use Committee.

344

345 **Skeletal examination**

346 To observe the skeletal systems, whole skeletons of WT and cKO littermates were stained
347 with alcian blue and alizarin red, as previously described (41, 42). The newborns were
348 skinned, eviscerated, and fixed in 95% ethanol. Intact skeletons were stained with 150 mg/ml
349 of alcian blue 8GX in 75% (vol/vol) ethanol/20% acetic acid for 24–48 hours, and excess
350 tissues were removed by 1–2% KOH digestion for 2–3 days. The skeletal preparations were
351 stained with 75 mg/ml of alizarin red S in 1% KOH for 24 hours and cleared in graded
352 glycerol solutions (43).

353

354 **Instability-induced OA model**

355 An OA model was created in 10-week-old mice by destabilizing the knee joint as previously
356 described (44). With the mice under general anesthesia, we destabilized the right knee joint
357 by transection of the medial collateral ligament and removing the cranial half of the medial
358 meniscus using a microsurgical technique (DMM). A sham operation was performed on the
359 left knee joint using the same approach, without ligament transection and meniscectomy. For
360 histological assessment, the mice were sacrificed, and the entire knee joint was dissected 8
361 weeks postoperatively.

362

363 **Age-associated OA model**

364 At 3, 4, 9, and 15 months of age, the mice were sacrificed, and their entire knee joints were
365 dissected to assess the spontaneous development of OA as a model of age-associated OA (44,
366 45).

367

368 **Human Cartilage Preparation**

369 Acquisition and use of patient tissues were approved by the institutional review board (IRB)
370 of Hokkaido University (approval number: 014-0144), and informed consent was obtained in
371 advance. Samples were from patients undergoing total knee arthroplasty for clinically and
372 radiologically diagnosed OA (n=5; age range 61–84 years, mean 72.4; male: female ratio
373 1:4). Age-matched control articular cartilage was from patients undergoing total hip
374 arthroplasty for femoral neck fracture with no history of joint disease (n=5; age range 45–88
375 years, mean 61.2 years; male: female ratio 3:2). Each cartilage specimen was evaluated
376 macroscopically by at least two veteran doctors to ensure that it had not suffered damage or
377 degeneration and was treated within 9 hours of harvest in the operating room. Immediately
378 upon receipt, isolated human cartilage was homogenized with a Polytron blender
379 (Kinematica, Luzern, Switzerland), and then cold ethanol was added to separate the protein
380 and lipid fractions.

381

382 **Total cartilage glycomic analysis**

383 N-glycans were released directly using cartilage lysates following deglycosylation by
384 overnight treatment with peptide N-glycanase F (PNGase F, 2U) (Roche, Switzerland). The
385 supernatants containing GSLs and fOSs were dried with a centrifugal evaporator. GSL-
386 glycans were isolated by enzymatic digestion using EGCase I (Takara Bio Inc. Japan),
387 whereas fOSs were recovered from an EGCase I-free fraction (46). Cartilage lysate was
388 delipidated and digested by GAG disaccharides (47). Extracted glycoproteins were subjected
389 to BEP for O-glycan analysis. Detailed procedures and materials are provided elsewhere (48).
390 N-glycans, fOSs, GAGs, and GSL-glycans were subjected to glycoblotting (49). Purified N-
391 glycans, fOSs, O-glycans, and GSL-glycan solutions were mixed with 2,5-dihydrobenzoic
392 acid and subjected to Matrix-assisted laser desorption/ionization-time of flight mass

spectrometry (MALDI-TOF MS). 2AB-labeled GAG disaccharides were analyzed by HPLC. The glycan compositions were manually determined by conducting database searches (i.e., a compositional search of the UniCarbKB database (http://www.unicarbkb.org/query) for fOSs and N- and O-glycans and of the SphinGOMAP database (http://www.sphingomap.org/) for GSL-glycans). All previously deposited GSL-glycans in the SphinGOMAP database were extracted and compiled as an in-house database to allow searching by the m/z value and/or composition. The absolute quantification was obtained by comparative analyses between the MS signal areas derived from each glycan and the internal standard.

Statistics

All data in this study are presented as the mean □ standard deviation and were repeated at least three times unless otherwise indicated. Data analysis was performed using GraphPad Prism 9 software version 9.4.1 (GraphPad Software, Inc., San Diego, CA, USA), and the Welch *t*-test/Welch analysis of variance with subsequent use of the Tukey–Kramer multiple comparison tests were used to determine significant differences between the groups. *P*-values <0.05 were considered significant. JMP Pro version 16.2.0 (SAS Institute, Cary, NC, USA) was used to reveal the relationships between each subject of sub glycomes; we performed principal component analysis (PCA) and hierarchical cluster analysis.

Study approval

Acquisition and use of patient tissues were approved by the institutional review board (IRB) of Hokkaido University (approval number: 014-0144), and informed consent was obtained in advance. All animal studies were performed according to established ethical guidelines approved by the local animal care committee.

418 **Data availability**

419 All data reported in this paper is available from the corresponding author upon request. This
420 paper does not report original code. Any additional information required to reanalyze the data
421 reported in this paper is available from the lead contact upon request.

422

423 **ACKNOWLEDGMENTS**

424 We thank the Iwasaki laboratory members for technical support, J. Gu (Tohoku
425 Pharmaceutical University) for the Flox-α1,6 fucosyltransferase (*Fut8*) mouse, Y. Kobayashi
426 (J-OIL MILLS, Inc.) for PhoSL-lectin. This work was funded by the Japan Society for the
427 Promotion of Science KAKENHI (Grant-in-Aid for Challenging Exploratory Research:
428 funding numbers: 16K15650, 19K22672 [to NI]; Grant-in-Aid for Research (B): funding
429 numbers: 22H03917 [to TO]; and Grant-in-Aid for Early-Career Scientists: funding number:
430 19K18516 [to KH]) and AMED (Grant Number JP22zf01270004h0002 [to NI, TO, KH]).

431

432 **AUTHOR CONTRIBUTIONS**

433 Conceptualization: NI
434 Methodology: KH, TO
435 Investigation: KH, TO, HH, JF, DM, MM, NI
436 Visualization: KH, HH
437 Funding acquisition: KH, NI, TO
438 Project administration: KH, TO, NI
439 Supervision: TO, NI
440 Writing – original draft: KH, TO
441 Writing – review & editing: KH, TO, HH, JF, DM, MM, NI

442

443 **CONFLICT-OF-INTEREST STATEMENT:** The authors have declared that no conflict of
444 interest exists.
445
446
447
448 **References**

449 1. Grillet B, et al. Matrix metalloproteinases in arthritis: towards precision medicine. *Nat.*
450 *Rev. Rheumatol.* [published online ahead of print: May 2023]; doi:10.1038/s41584-023-
451 00966-w
452 2. Safiri S, et al. Global, regional and national burden of osteoarthritis 1990-2017: a
453 systematic analysis of the Global Burden of Disease Study 2017. *Ann. Rheum. Dis.*
454 2020;79(6):819–828.
455 3. Thorstensson CA, et al. Natural course of knee osteoarthritis in middle-aged subjects with
456 knee pain: 12-year follow-up using clinical and radiographic criteria. *Ann. Rheum. Dis.*
457 2009;68(12):1890–1893.
458 4. Huey DJ, Hu JC, Athanasiou KA. Unlike bone, cartilage regeneration remains elusive.
459 *Science* 2012;338(6109):917–921.
460 5. Glyn-Jones S, et al. Osteoarthritis. *Lancet* [published online ahead of print: March 3,
461 2015]; doi:10.1016/S0140-6736(14)60802-3
462 6. Chu CR. Defining Pre-Osteoarthritis Is Key to Prevention. *Cartilage* 2016;7(2):204.
463 7. Mahmoudian A, et al. Early-stage symptomatic osteoarthritis of the knee - time for
464 action. *Nat. Rev. Rheumatol.* 2021;17(10):621–632.
465 8. Henrotin Y. Osteoarthritis in year 2021: biochemical markers. *Osteoarthritis Cartilage*
466 2021;S1063-4584(21)00960–2.

467 9. Vignon E, et al. Screening of degradative enzymes from articular cartilage in
468 experimental osteoarthritis. *Clin. Rheumatol.* 1987;6(2):208–214.

469 10. Brew CJ, et al. Gene expression in human chondrocytes in late osteoarthritis is changed
470 in both fibrillated and intact cartilage without evidence of generalised chondrocyte
471 hypertrophy. *Ann. Rheum. Dis.* 2010;69(1):234–240.

472 11. Otero M, et al. Human chondrocyte cultures as models of cartilage-specific gene
473 regulation. *Methods Mol. Biol. Clifton NJ* 2012;806:301–336.

474 12. Goldring MB. Chondrogenesis, chondrocyte differentiation, and articular cartilage
475 metabolism in health and osteoarthritis. *Ther. Adv. Musculoskelet. Dis.* 2012;4(4):269–
476 285.

477 13. van Meurs JB, et al. Kinetics of aggrecanase- and metalloproteinase-induced
478 neoepitopes in various stages of cartilage destruction in murine arthritis. *Arthritis*
479 *Rheum.* 1999;42(6):1128–1139.

480 14. Matsuhashi T, et al. Alteration of N-glycans related to articular cartilage deterioration
481 after anterior cruciate ligament transection in rabbits. *Osteoarthritis Cartilage*
482 2008;16(7):772–778.

483 15. Urita A, et al. Alterations of high-mannose type N-glycosylation in human and mouse
484 osteoarthritis cartilage. *Arthritis Rheum.* 2011;63(11):3428–3438.

485 16. Snelling S, et al. A gene expression study of normal and damaged cartilage in
486 anteromedial gonarthrosis, a phenotype of osteoarthritis. *Osteoarthr. Cartil. OARS*
487 *Osteoarthr. Res. Soc.* 2014;22(2):334–343.

488 17. Kobayashi Y, et al. A novel core fucose-specific lectin from the mushroom Pholiota
489 squarrosa. *J. Biol. Chem.* 2012;287(41):33973–33982.

490 18. Wu W, et al. Sites of collagenase cleavage and denaturation of type II collagen in aging
491 and osteoarthritic articular cartilage and their relationship to the distribution of matrix
492 metalloproteinase 1 and matrix metalloproteinase 13. *Arthritis Rheum.*
493 2002;46(8):2087–2094.

494 19. Song R-H, et al. Aggrecan degradation in human articular cartilage explants is mediated
495 by both ADAMTS-4 and ADAMTS-5. *Arthritis Rheum.* 2007;56(2):575–585.

496 20. Malfait A-M, et al. Inhibition of ADAM-TS4 and ADAM-TS5 prevents aggrecan
497 degradation in osteoarthritic cartilage. *J. Biol. Chem.* 2002;277(25):22201–22208.

498 21. Aigner T, et al. Anabolic and catabolic gene expression pattern analysis in normal versus
499 osteoarthritic cartilage using complementary DNA-array technology. *Arthritis Rheum.*
500 2001;44(12):2777–2789.

501 22. Karsdal MA, et al. Cartilage degradation is fully reversible in the presence of
502 aggrecanase but not matrix metalloproteinase activity. *Arthritis Res. Ther.*
503 2008;10(3):R63.

504 23. Reimann I, Christensen SB, Diemer NH. Observations of reversibility of
505 glycosaminoglycan depletion in articular cartilage. *Clin. Orthop.* 1982;(168):258–264.

506 24. Yang Q, Wang L-X. Mammalian α-1,6-Fucosyltransferase (FUT8) Is the Sole Enzyme
507 Responsible for the N-Acetylglucosaminyltransferase I-independent Core Fucosylation
508 of High-mannose N-Glycans. *J. Biol. Chem.* 2016;291(21):11064–11071.

509 25. Toegel S, et al. Glycophenotyping of osteoarthritic cartilage and chondrocytes by RT-
510 qPCR, mass spectrometry, histochemistry with plant/human lectins and lectin
511 localization with a glycoprotein. *Arthritis Res. Ther.* 2013;15(5):R147.

512 26. Yu H, et al. Characterization of aberrant glycosylation associated with osteoarthritis

513 based on integrated glycomics methods. *Arthritis Res. Ther.* 2023;25(1):102.

514 27. Homan K, et al. Alteration of the Total Cellular Glycome during Late Differentiation of
515 Chondrocytes. *Int. J. Mol. Sci.* 2019;20(14):E3546.

516 28. Fujitani N, et al. Total cellular glycomics allows characterizing cells and streamlining
517 the discovery process for cellular biomarkers. *Proc. Natl. Acad. Sci. U. S. A.*
518 2013;110(6):2105–2110.

519 29. Yoshida Y, et al. Quantitative analysis of total serum glycome in human and mouse.
520 *Proteomics* 2016;16(21):2747–2758.

521 30. Furukawa J-I, et al. Impact of the Niemann-Pick c1 Gene Mutation on the Total Cellular
522 Glycomics of CHO Cells. *J. Proteome Res.* 2017;16(8):2802–2810.

523 31. Gao C, et al. Sensitivity of heterozygous α 1,6-fucosyltransferase knock-out mice to
524 cigarette smoke-induced emphysema: implication of aberrant transforming growth
525 factor-β signaling and matrix metalloproteinase gene expression. *J. Biol. Chem.*
526 2012;287(20):16699–16708.

527 32. Wang X, et al. Dysregulation of TGF-beta1 receptor activation leads to abnormal lung
528 development and emphysema-like phenotype in core fucose-deficient mice. *Proc. Natl.*
529 *Acad. Sci. U. S. A.* 2005;102(44):15791–15796.

530 33. Gonzalez DS, Jordan IK. The alpha-mannosidases: phylogeny and adaptive
531 diversification. *Mol. Biol. Evol.* 2000;17(2):292–300.

532 34. Ross KA, et al. Comparison of Three Methods to Quantify Repair Cartilage Collagen
533 Orientation. *Cartilage* 2013;4(2):111–120.

534 35. Glasson SS, et al. Deletion of active ADAMTS5 prevents cartilage degradation in a
535 murine model of osteoarthritis. *Nature* 2005;434(7033):644–648.

536 36. Stanton H, et al. Investigating ADAMTS-mediated aggrecanolysis in mouse cartilage.
537 *Nat. Protoc.* 2011;6(3):388–404.

538 37. Estes BT, et al. Isolation of adipose-derived stem cells and their induction to a
539 chondrogenic phenotype. *Nat. Protoc.* 2010;5(7):1294–1311.

540 38. Patwari P, et al. Ultrastructural quantification of cell death after injurious compression
541 of bovine calf articular cartilage. *Osteoarthr. Cartil. OARS Osteoarthr. Res. Soc.*
542 2004;12(3):245–252.

543 39. Rao X, et al. An improvement of the 2ˆ(-delta delta CT) method for quantitative real-
544 time polymerase chain reaction data analysis. *Biostat. Bioinforma. Biomath.*
545 2013;3(3):71–85.

546 40. Ovchinnikov DA, et al. Col2a1-directed expression of Cre recombinase in
547 differentiating chondrocytes in transgenic mice. *Genes. N. Y. N 2000* 2000;26(2):145–
548 146.

549 41. Yamada T, et al. Carminerin contributes to chondrocyte calcification during
550 endochondral ossification. *Nat. Med.* 2006;12(6):665–670.

551 42. Nakamichi Y, et al. Chondromodulin I is a bone remodeling factor. *Mol. Cell. Biol.*
552 2003;23(2):636–644.

553 43. Lufkin T, et al. Homeotic transformation of the occipital bones of the skull by ectopic
554 expression of a homeobox gene. *Nature* 1992;359(6398):835–841.

555 44. Matsui Y, et al. Accelerated development of aging-associated and instability-induced
556 osteoarthritis in osteopontin-deficient mice. *Arthritis Rheum.* 2009;60(8):2362–2371.

557 45. Stoop R, et al. Type II collagen degradation in spontaneous osteoarthritis in C57Bl/6 and

558 BALB/c mice. *Arthritis Rheum.* 1999;42(11):2381–2389.

559 46. Fujitani N, et al. Qualitative and quantitative cellular glycomics of glycosphingolipids
560 based on rhodococcal endoglycosylceramidase-assisted glycan cleavage, glycoblotting-
561 assisted sample preparation, and matrix-assisted laser desorption ionization tandem
562 time-of-flight mass spectrometry analysis. *J. Biol. Chem.* 2011;286(48):41669–41679.

563 47. Takegawa Y, et al. Simultaneous analysis of heparan sulfate, chondroitin/dermatan
564 sulfates, and hyaluronan disaccharides by glycoblotting-assisted sample preparation
565 followed by single-step zwitter-ionic-hydrophilic interaction chromatography. *Anal.*
566 *Chem.* 2011;83(24):9443–9449.

567 48. Furukawa J, et al. Quantitative O-Glycomics by Microwave-Assisted β-Elimination in
568 the Presence of Pyrazolone Analogues. *Anal. Chem.* 2015;87(15):7524–7528.

569 49. Furukawa J, et al. Comprehensive approach to structural and functional glycomics based
570 on chemoselective glycoblotting and sequential tag conversion. *Anal. Chem.*
571 2008;80(4):1094–1101.

572

573 **FIGURES**

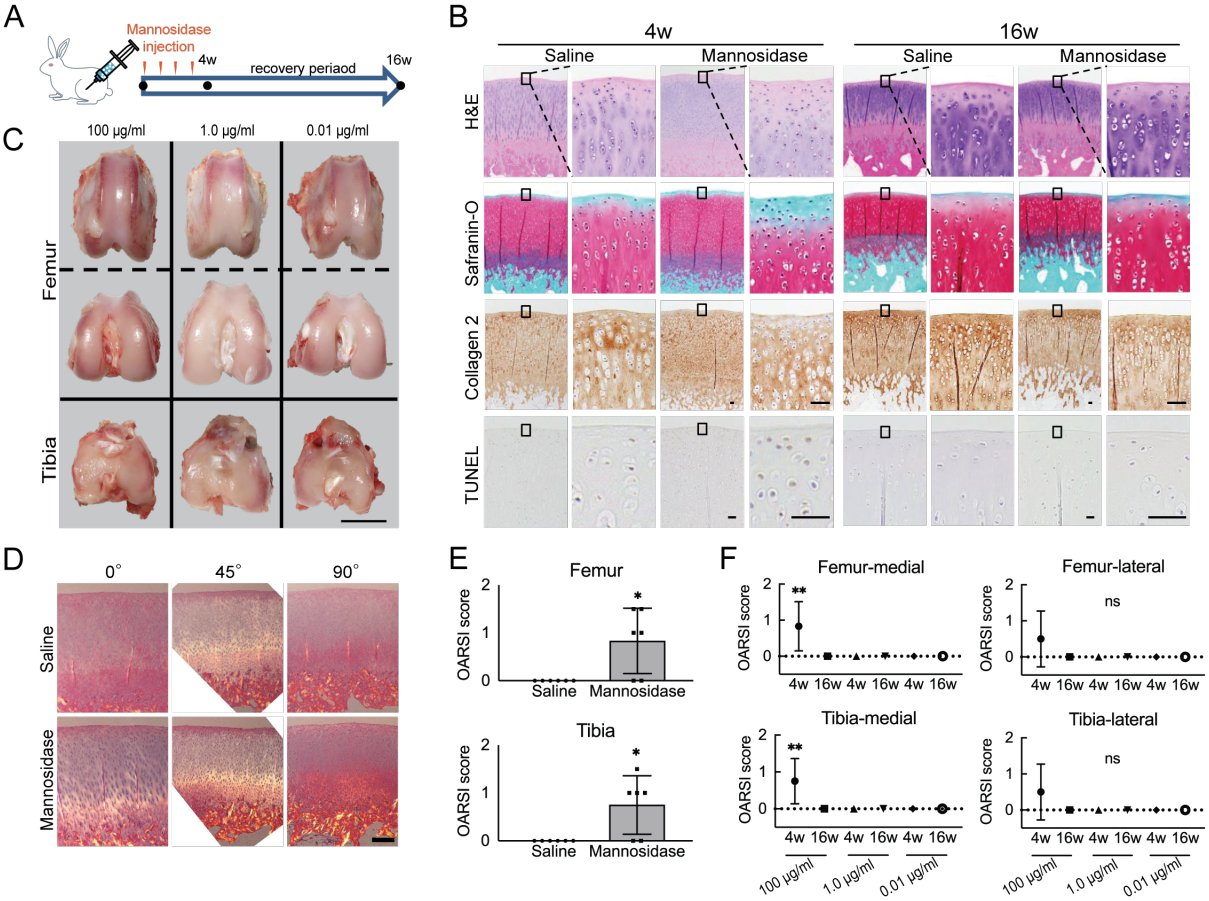

574

575 **Fig. 1. Effects of α-mannosidase injection in the knee joint in vivo.**

576 **(A)** Time course of intra-articular α-mannosidase injection and unloading. Red arrows
577 indicate the one-shot, intra-articular injection that was performed once a week. **(B)**
578 Histological evaluation of knee articular cartilage 4 weeks after intermittent α-mannosidase
579 infusion and 16 weeks after load removal. Scale bars, 50 μm. **(C)** Representative macroscopic
580 assessment of the articular cartilage using mannosidase concentration. Scale bar, 1 cm. **(D)**
581 Evaluation of the collagen orientation of reparative tissues at 4 weeks postoperatively.
582 Sections stained with HE was viewed under a polarized light microscope at multiple angles
583 (0°, 45°, and 90°). Scale bar, 200 μm. **(E)** OARSI scores at 4 weeks postoperatively on
584 sections from the knee joint (n = 6). **(F)** Tissue degeneration scores at each time point are
585 based on mannosidase concentration. Data are shown as mean ± standard deviation. *P <

586 0.05, **$P < 0.01$ versus the saline group in (E), and versus 4 weeks in (F). In (E), the Welch
587 t-test was used for statistical analysis. In (F), n = 6 rabbits per group. One-way analysis of
588 variance with Tukey's multiple comparison test was used to perform statistical analysis. HE,
589 hematoxylin and eosin; OARSI, Osteoarthritis Research Society International; TUNEL,
590 terminal deoxynucleotidyl transferase dUTP nick end labeling.

591

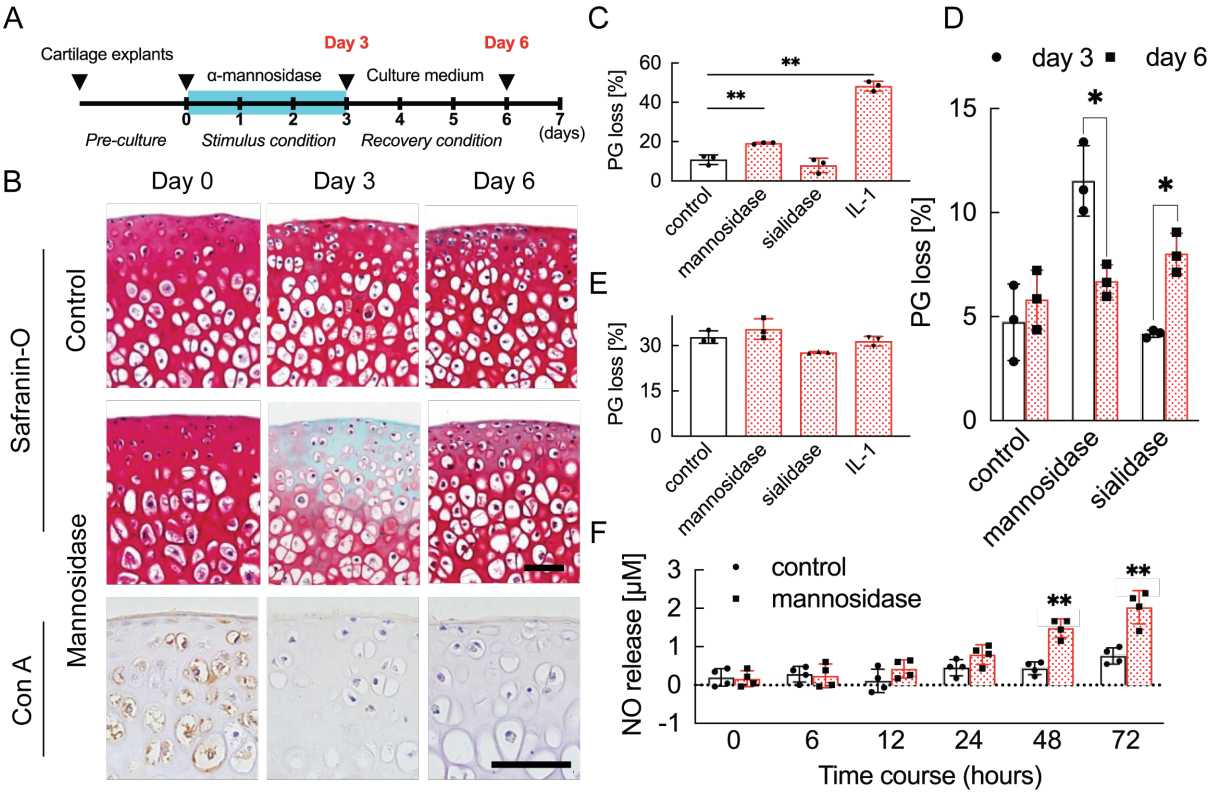

Fig. 2. Cartilage degradation induced by mannosidase stimulation.

(A) Schematic diagram of the procedures used to establish the early OA model before irreversible and progressive destruction of articular cartilage. **(B)** Mannosidase-treated cartilage stained with Safranin O and Con A. The distribution of high-mannose type N-glycans is decreased in mannosidase-induced degraded mouse cartilage. Scale bars, 50 μm. **(C), (D)** PG release after exposure to mannosidase (C) and recovery after its removal from cultured cartilage grafts (D). **(E)** To investigate the non-chondrocyte-mediated release of fragments, PG loss was measured in cartilage explants that had undergone freeze-thaw cycles. **(F)** Sequential NO released into media measured as concentrations of nitrite for cartilage explants stimulated with mannosidase. Data are shown as mean ± standard deviation (s.d.). $*P < 0.05$, $**P < 0.01$ versus the control group in **c**, **e,** and (F), and versus day 3 in (D). In (C) and (E), n = 3 samples (six mice) per group. One-way ANOVA with the Tukey multiple comparison test was used to perform statistical analysis. In (D), n = 12 mice in each group and n = 3 samples (six mice) at each time point. In (F), n = 16 mice at each time point

607 and n = 4 samples (eight mice) per group. In (D) and (F), two-way ANOVA with the Sidak

608 multiple-comparisons test was used to perform statistical analysis. Con A, concanavalin A;

609 NO, nitric oxide; ANOVA, analysis of variance; PG, proteoglycan.

610

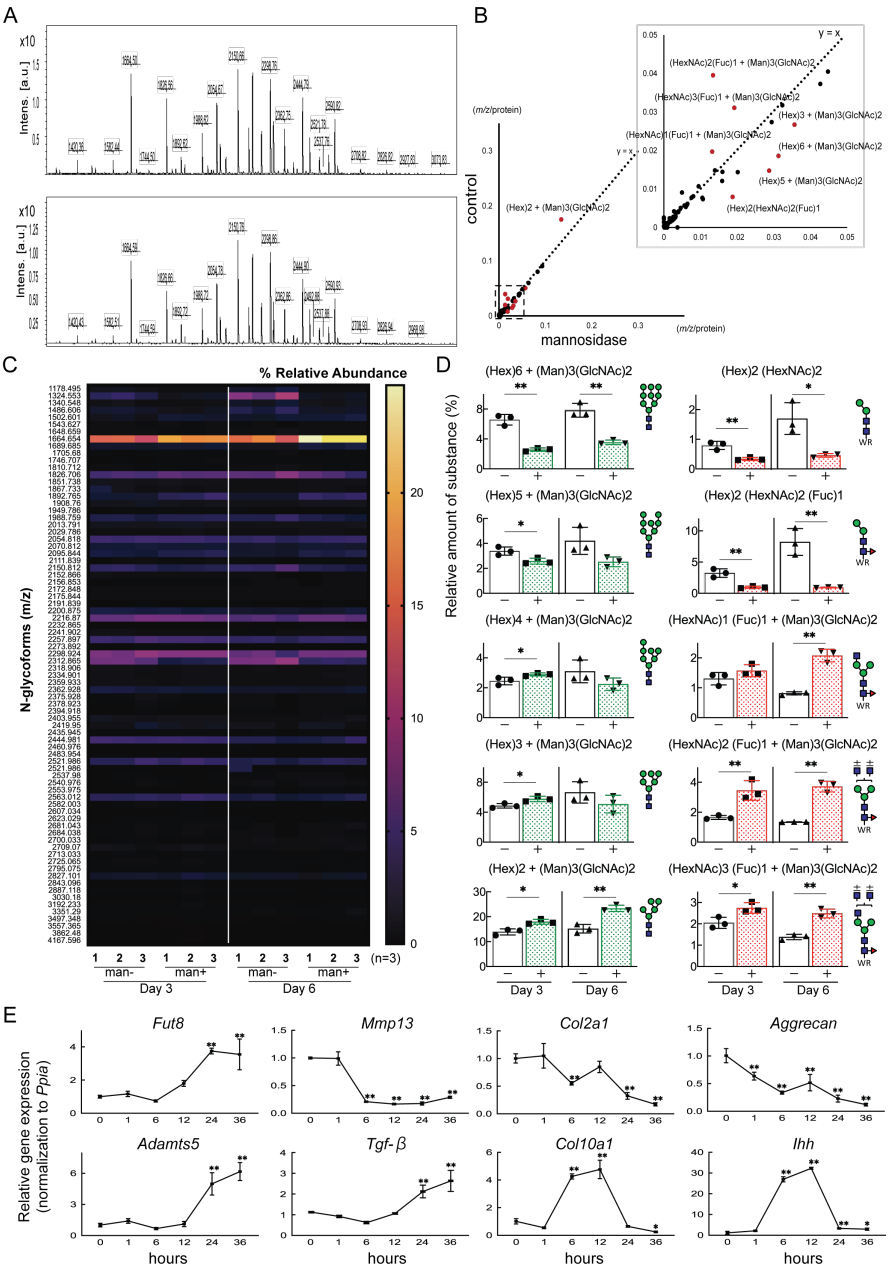

Fig. 3. Cartilage N-glycomes.

(A) MALDI-TOF MS spectra showing the quantitative N-glycan profiles of cartilage before (upper) and after (lower) mannosidase treatment. **(B)** Scatter plot of the changes in *m/z* per protein abundance in the mannosidase (x-axis) and control (y-axis) N-glycan structures. The red dots indicate the top 10 N-glycan structures based on the deviation from the y = x line. **(C)** Heatmap of N-glycome showing differential N-glycan expression in the mannosidase (man+) group versus the control (man-) group. **(D)** N-glycans altered by mannosidase were

619 corefucosylated glycans and high-mannose type N-glycans. (**E)** RT-PCR expression analysis
620 of marker genes in organ culture of cartilage with mannosidase. Data are shown as mean ±
621 standard deviation. *$P < 0.05$, **$P < 0.01$ versus the control group in (D), and versus 0 hours
622 in (E). In (D) and (E), n = 3 samples (six mice) per group. In (D), unpaired t-tests were used
623 to perform statistical analyses. In (E), one-way ANOVA with the Dunnett multiple
624 comparison test was used to perform statistical analysis. MALDI-TOF MS, matrix-assisted
625 laser desorption/ionization-time of flight mass spectrometry; ANOVA, analysis of variance;
626 RT-PCR, real-time polymerase chain reaction.

627

628

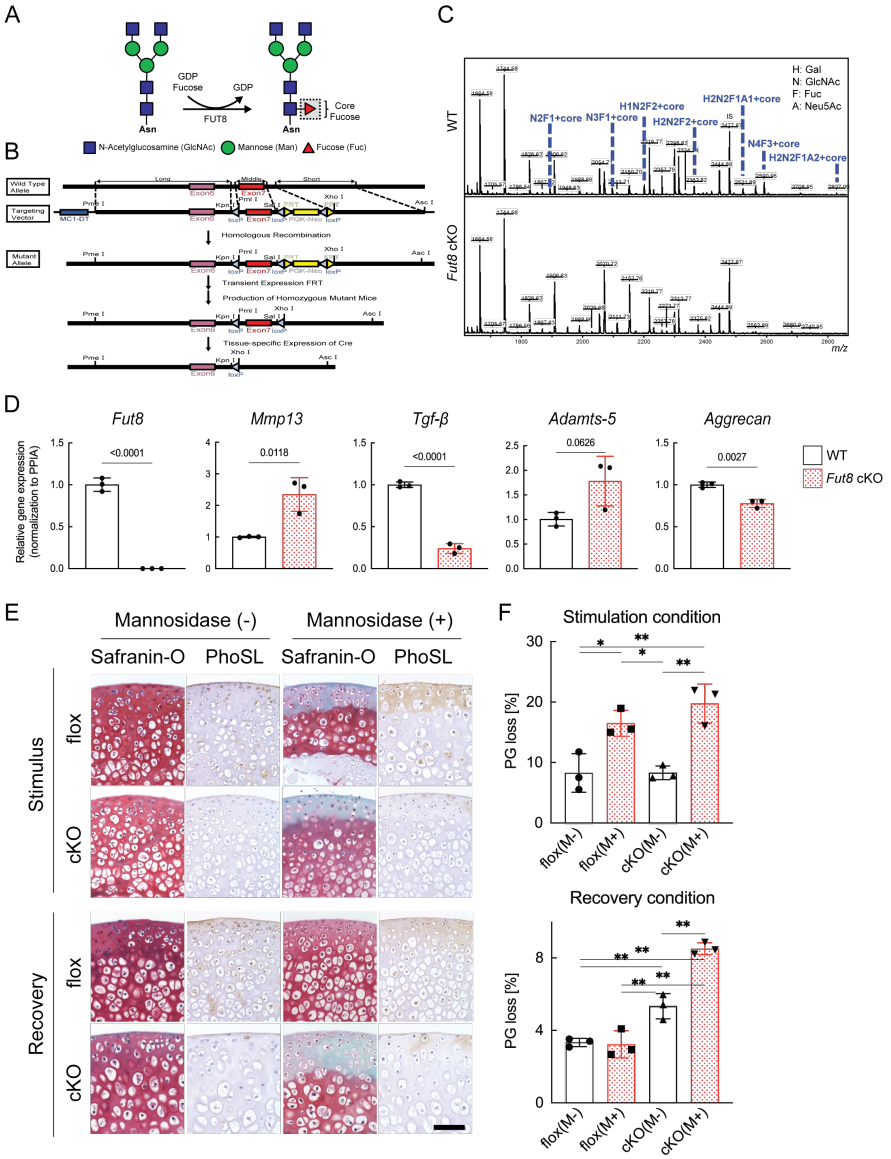

629

630 **Fig. 4. Loss of resilience due to FUT8 deficiency in cartilage.**

631 **(A)** Biological reaction of FUT8. FUT8 transfers fucose to the innermost GlcNAc residue of

632 complex N-glycans via α1,6-linkage (corefucosylation). **(B)** Targeted disruption of *Fut8*

633 locus. The *Fut8* gene (WT allele; top), targeting vector (middle), and disrupted *Fut8* locus

634 (mutant allele; bottom). Schematic representation of the *Fut8*-targeting strategy and Cre-

635 mediated recombination of the *Fut8*^{loxP} allele. **(C)** MALDI-TOF MS mass spectra of N-

636 glycans from WT and *Fut8* cKO mice. The corefucosylation levels in cartilage were

637 decreased and undetectable in *Fut8* cKO mice. (**D)** Gene profile in chondrocytes isolated
638 from *Fut8* cKO mice. The expression levels of these genes in WT cells were set to 1. PPIA,
639 peptidylprolyl isomerase A. (**E)** Histological findings in cartilage explants from *Fut8* cKO
640 mice and their floxed littermates, cultured with mannosidase and subjected to Safranin O
641 staining and PhoSL lectin staining. Scale bar, 50 μm. (**F)** PG release in cultured cartilage
642 explants from *Fut8* cKO mice and their floxed littermates. Data are shown as mean ±
643 standard deviation. In (E), n = 3 samples (six mice) per group. *$P < 0.05$, **$P < 0.01$ versus
644 the control group. One-way ANOVA, with the Tukey multiple comparison test, was used to
645 perform statistical analysis. MALDI-TOF MS, matrix-assisted laser desorption/ionization-
646 time of flight mass spectrometry; WT, wild-type; cKO, conditional knockout; PG,
647 proteoglycan; ANOVA, analysis of variance.

648

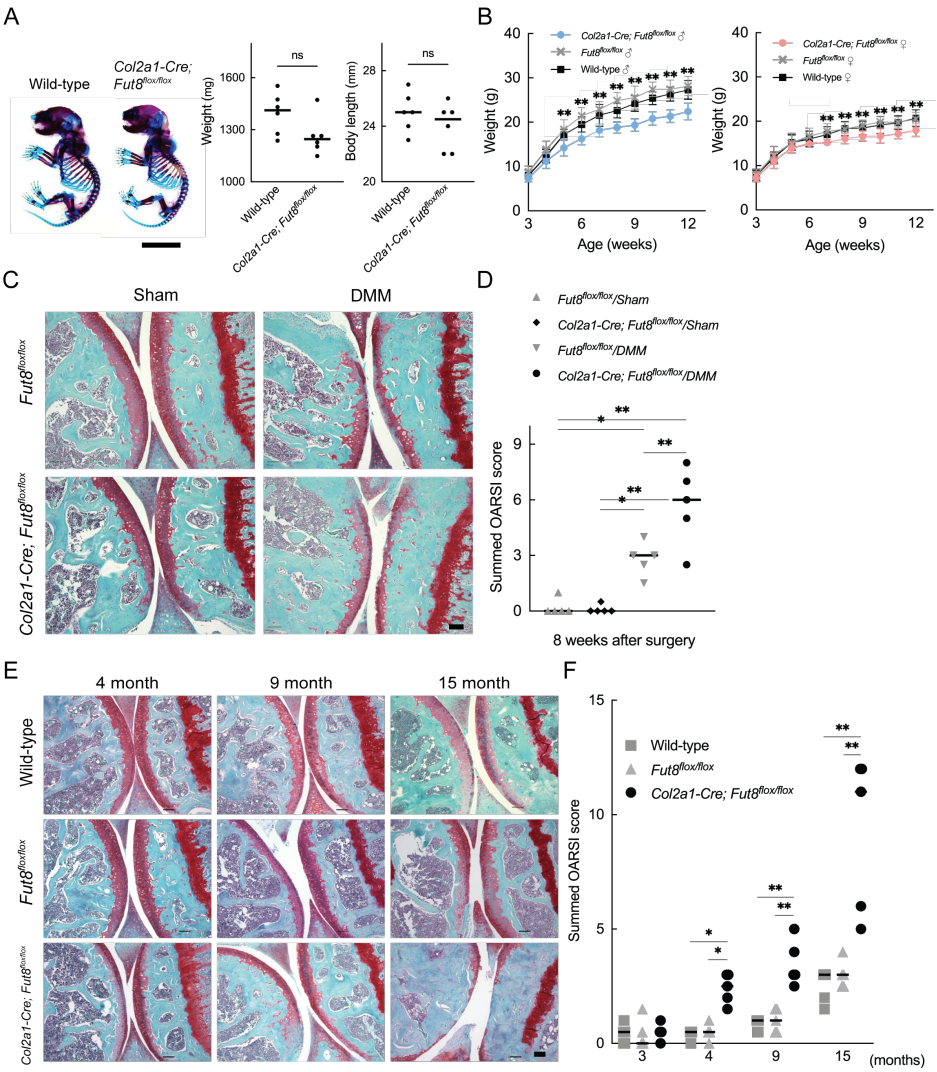

Fig. 5. OA acceleration in *Fut8* cKO mice.

(A) Double staining with alizarin red and alcian blue of the whole skeleton of wild-type and *Col2a1-Cre;Fut8*$^{flox/flox}$ cKO littermate embryos (newborn). Scale bars, 1 cm (left). Weight and body length of wild-type and cKO littermate embryos (right). **(B)** Growth curves determined by body weight in male (left) and female (right) wild-type mice and their cKO littermates. **(C)**, **(D)** Features of instability-induced OA in *Fut8*$^{flox/flox}$ (flox) mice and their cKO littermates at 8 weeks after surgery. Safranin O staining is shown for each mouse genotype. Scale bar, 100 μm (C). Summed histological scores for OA severity in the knee cartilage from flox and cKO mice, as determined using the OARSI scoring system, are shown (D). **(E)**, **(F)** Features of age-associated osteoarthritis in wild-type mice and their flox and

660 cKO littermates. Safranin O staining of the knee joint is shown for each mouse genotype at 3,
661 4, 9, and 15 months of age. Scale bar, 100 μm (E). The summed OARSI scores are shown (F).
662 Data are shown as mean ± standard deviation. In (A), the Welch t-test was used to perform
663 statistical analyses (n = 6 mice per group). In (B), n = 15 mice per group at each time point.
664 In (D) and (F), n = 5 mice per group at each time point. *$P < 0.05$, **$P < 0.01$ versus the
665 wild-type group in (B) and (F), and versus flox mice in (D). One-way ANOVA with the
666 Tukey multiple comparisons test (B), (D) and two-way ANOVA with the Tukey multiple
667 comparisons test (F) were used to perform statistical analysis. OA, osteoarthritis; cKO,
668 conditional knockout; OARSI, Osteoarthritis Research Society International. ANOVA,
669 analysis of variance; ns, not significant.

670

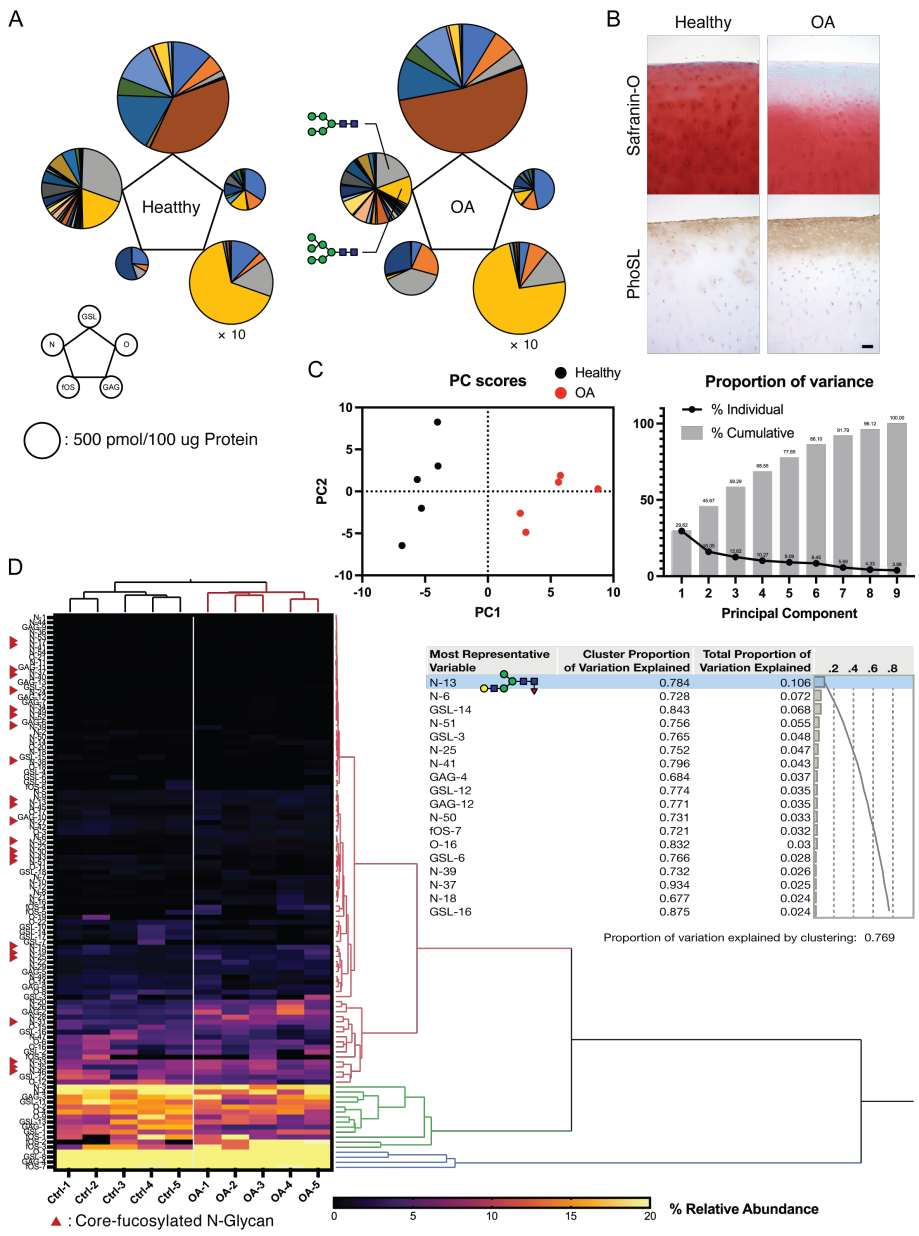

Fig. 6. Altered glycosylation of human Osteoarthritis (OA) cartilage based on comprehensive glycan analysis.

(A) Total glycome profiling of human OA cartilage. Pie charts at the vertices of the pentagon correspond to the glycan expression profiles of N-glycans, O-glycans, GSL-glycans, free oligosaccharides (fOS), and glycosaminoglycan (GAG). The size of each circle and its constituent colors reflect the absolute quantity of glycans (pmol/100 μg protein) and the glycan substructures, respectively. The sizes of the circles representing the GAG contents are increased by 10-fold. Each color indicates the estimated glycan structure and corresponds to

680 the respective glycan number listed in the S3 Table. (**B)** Expression of core fucose in healthy
681 and OA cartilage. Scale bar, 100 μm. (**C)** Principal component analysis (PCA) of a glycan
682 expression data set. Data points represent individual samples. The first principal component
683 (PC1) distinguishes healthy and OA samples. (**D)** Hierarchical cluster analysis results
684 showing cluster image display for total glycans with color gradient for relative glycan
685 expression and dendrogram for each glycan structure. Cluster summary of PCA on the
686 glycome are shown on the right. The most representative variable is (Hex)1 (HexNAc)1
687 (Fuc)1 + (Man)3(GlcNAc)2 that means the largest squared correlation with its cluster
688 component.
689
690